HHS Public Access

Author manuscript

Anal Biochem. Author manuscript; available in PMC 2022 October 07.

Published in final edited form as:

Anal Biochem. 2022 August 01; 650: 114712. doi:10.1016/j.ab.2022.114712.

Optimized quantitative PCR analysis of random DNA aptamer libraries

Keenan Pearson[a,b], **Caroline Doherty**[a,c], **Drason Zhang**[a], **Nicole A. Becker**[a], **L. James Maher III**[a,*]

[a]Department of Biochemistry and Molecular Biology, Mayo Clinic College of Medicine and Science, 200 First St. SW, Rochester, MN, 55905, USA

[b]Biochemistry and Molecular Biology Track, Mayo Clinic Graduate School of Biomedical Sciences, Mayo Clinic College of Medicine and Science, 200 First St. SW, Rochester, MN, 55905, USA

[c]Medical Scientist Training Program, Mayo Clinic Graduate School of Biomedical Sciences and Mayo Clinic Alix School of Medicine, Mayo Clinic College of Medicine and Science, 200 First St. SW, Rochester, MN, 55905, USA

Abstract

The quantitative polymerase chain reaction (qPCR) with detection of duplex DNA yield by intercalator fluorescence is a common and essential technique in nucleic acid analysis. We encountered unexpected results when applying standard qPCR methods to the quantitation of random DNA libraries flanked by regions of fixed sequence, a configuration essential for in vitro selection experiments. Here we describe the results of experiments revealing why conventional qPCR methods can fail to allow automated analysis in such cases, and simple solutions to this problem. In particular we show that renaturation of PCR products containing random regions is incomplete in late PCR cycles when extension fails due to reagent depletion. Intercalator fluorescence can then be lost at standard interrogation temperatures. We show that qPCR analysis of random DNA libraries can be achieved simply by adjusting the step at which intercalator fluorescence is monitored so that the yield of annealed constant regions is detected rather than the yield of full duplex DNA products.

1. Introduction

The quantitative polymerase chain reaction (qPCR) is a highly sensitive and specific method for detection of DNA. A typical thermal cycler protocol for qPCR involves steps to denature

*Corresponding author. maher@mayo.edu (L.J. Maher).

Author contributions

Project conception and manuscript preparation: KP, LJM.
Experiments: KP, CD, DZ.
Data analysis: KP, NAB, LJM.
Manuscript composition: KP, LJM.

Appendix A. Supplementary data

Supplementary data to this article can be found online at https://doi.org/10.1016/j.ab.2022.114712.

the DNA (~95 °C), anneal primers (near the denaturation temeperature, T_m, values for the primers involved), and extend the primers using thermostable DNA polymerase to form duplex DNA (~72 °C) (Fig. 1A). The temperature of the annealing step can be optimized to balance specificity of target amplification and PCR efficiency. The temperature of the extension step is typically based on the optimum temperature for the relevant DNA polymerase enzymatic activity [1–4]. When primer T_m values are sufficiently high, a two-step thermal cycler protocol can be employed by combining annealing and extension steps. For the real-time detection of PCR products, several methods have been developed to monitor product formation. The simplest methods involve quantitation of duplex DNA products by automated monitoring of DNA duplex-dependent intercalator fluorescence using ethidium bromide [5,6], or SYBR Green I [7–9]. The more sophisticated Taqman approach exploits DNA polymerase-dependent fluorogenic cleavage of specific labeled oligonucleotide probes hybridized to PCR products [10,11].

Directed evolution methods such as Systematic Evolution of Ligands by EXponential enrichment (SELEX) utilize vast pools of nucleic acid sequences synthesized with central random regions flanked by fixed primer sequences for PCR amplification (Fig. 1C, top). Since its development [12,13] in vitro selection has been routinely used to identify nucleic acid aptamers with desired affinities or activities [14]. In vitro selection typically exploits DNA libraries where the random region length is maximized and the fixed primer region length is minimized to allow for the greatest diversity of possible folded nucleic acid shapes. This implies that T_m values of primers used to amplify the libraries are often relatively low. Such designs are thus less amenable to two-step thermal cycler protocols.

It is often desirable to apply qPCR to quantitative analysis of random DNA libraries during in vitro selection. This may be used to track progress of library recovery throughout the selection as an indirect indicator of sequence enrichment. Fluorophores are often included in the random DNA libraries to facilitate detection, but qPCR allows for direct quantitation of fully intact DNA molecules. Here we describe unexpected challenges associated with qPCR analysis of DNA libraries containing such random regions, and report optimization strategies to resolve the issues.

2. Results and discussion

Using intercalator-based qPCR methods with standard measurement of intercalator fluorescence at the conclusion of each extension step (Fig. 1A), the typical qPCR profile for an 80-nucleotide (nt) DNA template with 20-nt primers [here denoted as a 20(40)20 template; Fig. 1B, top] is shown in Fig. 1B, bottom.

In vitro selection libraries in our laboratory are often analyzed using qPCR with SYBR Green detection to monitor recoveries of DNA pools at various stages selection. We applied this method to an 80-nt DNA library comprising a central 40-nt random region flanked by 20-nt fixed regions for PCR amplification [here denoted as a 20(N_{40})20 template; Fig. 1C, top]. Despite using the identical qPCR protocol as for the 20(40)20 template, we were confronted by the puzzling qPCR profile shown in Fig. 1C, bottom. Rather than the expected sigmoid pattern required for automated fitting and quantification cycle (C_q) determination,

the relative fluorescence value peaks but then drops inexplicably over subsequent PCR cycles. Literature review indicates that this problem has also been observed in other SELEX-based DNA libraries [15]. This result prevents reliable automated recovery quantitation and we here describe such curves as “uninterpretable non-sigmoid curves.” We undertook an analysis to understand and mitigate the problem.

We first observed that libraries of the structure 27(N_{40})26 gave aberrant qPCR profiles reminiscent of those obtained for 20(N_{40})20 libraries, but with less severe signal decline at late PCR cycles. We refer to such cases as “poorly interpretable partial sigmoid curves” (Table 1 and Supplemental Fig. S1). This apparent dependence of qPCR profile on flanking primer length led us to test the possibility of improving the uninterpretable non-sigmoid qPCR profile of 20(N_{40})20 libraries by substituting longer primers (initially with 5’ overhangs) as shown in Fig. 2A. Interestingly, the resulting qPCR profiles for the problematic 20 (N_{40})20 library were somewhat improved (Fig. 2B, compare solid and dashed lines) and Table 1). Because increasing primer T_m values contribute to the overall stability of the resulting duplex DNA products after extension (where the fluorescent signal is typically interrogated in automated systems), we also tested two sets of forward/reverse 27-nt primers with different T_m values (60.6/60.1 °C and 64.4/64.8 °C, respectively). Interestingly, the primer set with the higher T_m values showed further improvement in qPCR curve profile (Fig. 2C), yielding a poorly interpretable partial sigmoid result rather than an uninterpretable non-sigmoid result (Table 1).

These findings motivated us to reconsider how the length of stable duplex DNA (which determines the intensity of fluorescent readout) depends on the point of detection in the PCR cycle. We modified the thermal cycler protocol to interrogate SYBR Green fluorescence at three points in the PCR cycle: after anneal, extend, or an appended cool step (Fig. 3A). Interrogation after the extend step again resulted in an uninterpretable non-sigmoid qPCR profile, while interrogation after the cool step strongly improved interpretability of the profile. Importantly, interrogation after the anneal step resulted in an easily interpretable sigmoid qPCR profile (Fig. 3B). In fact, we find that alteration of the qPCR protocol to interrogate fluorescence after the anneal step is sufficient to generate normal and interpretable qPCR profiles from templates with random regions, without any need to add an additional cool step.

Based on these results, we propose a model to explain the drastic loss of fluorescent signal observed for later rounds of qPCR amplification involving random DNA libraries interrogated after the extend step (Fig. 3C). During early, reagent-rich PCR cycles, fluorescent detection after the extend step accurately detects stable, full-length duplexes created by complete primer extension. The situation is dramatically different in late PCR cycles when primers are depleted [16]. Under those circumstances the PCR cycle degenerates into simple alternation between denaturation and renaturation of existing DNA molecules without new primer extension. When a single DNA sequence is present (as in qPCR analysis of a unique sequence), complete DNA renaturation is efficient and intercalation-dependent fluorescent signal remains constant. In contrast, for complex template populations containing mixed central sequences, repeated denaturation and renaturation without primer extension promotes annealing only of the fixed flanking

sequences in the templates. Without primer extension the complex internal sequences reanneal poorly with their complements present at vanishingly low concentration. Furthermore, the fixed flanking sequences in the templates do not stably anneal because the T_m values for these regions are substantially lower than the temperature of the extension step, causing loss of detected fluorescence. These late PCR products thus contain large unpaired central regions after the anneal step, no annealed products after the extend step, and only flanking duplex regions after the cool step of the cycle (Fig. 3C). Because the yield of duplex DNA afforded either by primer binding (early) or by annealing of fixed flanking sequences (late) is proportional to the yield of amplified templates, fluorescent detection at the anneal step (Fig. 3A) provides a convenient and general solution to qPCR analysis of DNA libraries involving random regions.

While there may be manual approaches to extracting threshold qPCR values from early portions of qPCR curves that are otherwise uninterpetable, such curves cannot be processed by standard automated routines. We have therefore completely avoided the issue by implementing simple experimental changes. Synthesis of longer PCR primers can somewhat improve qPCR curves, but this involves the design and purchase of additional reagents specific for qPCR of the random DNA aptamer libraries. Instead, simply adjusting the thermal cycler protocol to interrogate fluorescence after the anneal step provides general and optimal results.

3. Materials and methods

3.1. DNA primers and templates

DNA oligonucleotide primers and templates containing fixed or fixed and random sequences were purchased from Integrated DNA Technologies with standard desalting (Coralville, IA). DNA templates containing random regions (LJM-6014, LJM-6236, LJM-6472, or fixed sequences: LJM-6197, LJM-6271, LJM-6593, sequences provided in Supplemental Table S1) were added to qPCR mixtures at final concentrations of 1 nM, 100 pM, 10 pM, and 1 pM to allow generation of standard curves (Supplemental Fig. S1). Primers (LJM-5505, LJM-6160, LJM-6239, LJM-6240, LJM-6474, LJM-6520, LJM-6521, LJM-6626, LJM-6627, LJM-6647, LJM-6648, LJM-6649, LJM-6650; sequences provided in Supplemental Table S2) were added to qPCR mixtures at a final concentration of 0.5 μM.

3.2. qPCR

qPCR mixtures (30 μL) were performed with the following reagent volumes: 15 μL PerfeCTa SYBR Green FastMix for IQ (Quantabio, 95071–012), 3 μL 5 μM forward primer (0.5 μM final concentration), 3 μL 5 μM reverse primer (0.5 μM final concentration), 7.5 μL water, 1.5 μL template (standard curves contained final template concentrations of 1 nM, 100 pM, 10 pM, and 1 pM). Samples were transferred to a CFX96 Touch Deep Well Real-Time PCR Detection System (Bio-Rad Laboratories, 1854095) and subjected to thermal cycling using a protocol of 95 °C, 30s; 40 × (95 °C 15s, 51 °C 30s, 72 °C 30s, 48 °C 30s), and interrogating SYBR Green fluorescence after the anneal (51 °C, 30s), extension (72 °C, 30s), and cool (48 °C, 30s) steps of each cycle. Raw fluorescence data were then analyzed using CFX Maestro™ software.

Supplementary Material

Refer to Web version on PubMed Central for supplementary material.

Acknowledgments

The authors thank members of the Maher lab for their assistance.

Funding

This work was supported by NIH grant GM128579 (L.J.M.), by the Mayo Clinic Graduate School of Biomedical Sciences, and by NIH grant T32GM065841 (Medical Scientist Training Program of the Mayo Clinic Graduate School of Biomedical Sciences and Mayo Clinic Alix School of Medicine).

References

[1]. Saghatelyan A, Panosyan H, Trchounian A, Birkeland NK, Characteristics of DNA polymerase I from an extreme thermophile, Thermus scotoductus strain K1, Microbiol. 10 (2021) e1149.

[2]. Hogrefe HH, Cline J, Lovejoy AE, Nielson KB, DNA polymerases from hyperthermophiles, Methods Enzymol. 334 (2001) 91–116. [PubMed: 11398488]

[3]. Lawyer FC, Stoffel S, Saiki RK, Chang SY, Landre PA, Abramson RD, Gelfand DH, High-level expression, purification, and enzymatic characterization of full-length Thermus aquaticus DNA polymerase and a truncated form deficient in 5’ to 3’ exonuclease activity, PCR Methods Appl. 2 (1993) 275–287. [PubMed: 8324500]

[4]. Chien A, Edgar DB, Trela JM, Deoxyribonucleic acid polymerase from the extreme thermophile Thermus aquaticus, J. Bacteriol 127 (1976) 1550–1557. [PubMed: 8432]

[5]. Higuchi R, Fockler C, Dollinger G, Watson R, Kinetic PCR analysis: real-time monitoring of DNA amplification reactions, Biotechnology 11 (1993) 1026–1030. [PubMed: 7764001]

[6]. Higuchi R, Dollinger G, Walsh PS, Griffith R, Simultaneous amplification and detection of specific DNA sequences, Biotechnology 10 (1992) 413–417. [PubMed: 1368485]

[7]. Cao H, Shockey JM, Comparison of TaqMan and SYBR Green qPCR methods for quantitative gene expression in tung tree tissues, J. Agric. Food Chem 60 (2012) 12296–12303. [PubMed: 23176309]

[8]. Giglio S, Monis PT, Saint CP, Demonstration of preferential binding of SYBR Green I to specific DNA fragments in real-time multiplex PCR, Nucleic Acids Res. 31 (2003) e136. [PubMed: 14602929]

[9]. Wittwer CT, Herrmann MG, Moss AA, Rasmussen RP, Continuous fluorescence monitoring of rapid cycle DNA amplification, Biotechniques 22 (130–131) (1997) 134–138.

[10]. Heid CA, Stevens J, Livak KJ, Williams PM, Real time quantitative PCR, Genome Res. 6 (1996) 986–994. [PubMed: 8908518]

[11]. Holland PM, Abramson RD, Watson R, Gelfand DH, Detection of specific polymerase chain reaction product by utilizing the 5’——3’ exonuclease activity of Thermus aquaticus DNA polymerase, Proc. Natl. Acad. Sci. U. S. A 88 (1991) 7276–7280. [PubMed: 1871133]

[12]. Tuerk C, Gold L, Systematic evolution of ligands by exponential enrichment: RNA ligands to bacteriophage T4 DNA polymerase, Science 249 (1990) 505–510. [PubMed: 2200121]

[13]. Ellington AD, Szostak JW, In vitro selection of RNA molecules that bind specific ligands, Nature 346 (1990) 818–822. [PubMed: 1697402]

[14]. Nimjee SM, White RR, Becker RC, Sullenger BA, Aptamers as therapeutics, Annu. Rev. Pharmacol. Toxicol 57 (2017) 61–79. [PubMed: 28061688]

[15]. Kolm C, Cervenka I, Aschl UJ, Baumann N, Jakwerth S, Krska R, Mach RL, Sommer R, DeRosa MC, Kirschner AKT, et al. , DNA aptamers against bacterial cells can be efficiently selected by a SELEX process using state-of-the art qPCR and ultra-deep sequencing, Sci. Rep 10 (2020) 20917. [PubMed: 33262379]

[16]. Jansson L, Hedman J, Challenging the proposed causes of the PCR plateau phase, Biomol Detect Quantif 17 (2019) 100082. [PubMed: 30886826]

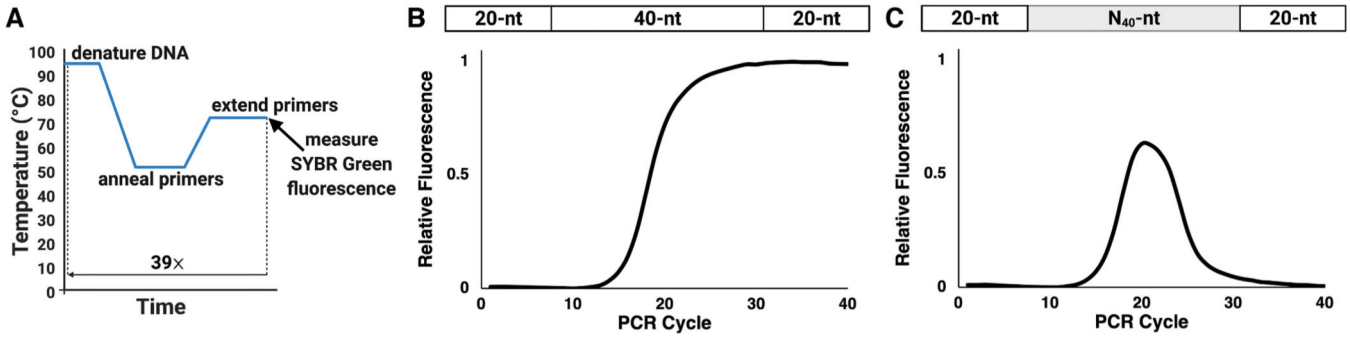

Fig. 1.

A) Schematic of typical qPCR thermal cycle based on SYBR Green fluorescence detection after the primer extension step. B) Example of a typical qPCR profile for a defined 40-nucleotide (nt) DNA sequence flanked by two 20-nt fixed primer regions showing results consistent with expectation. C) Example of a typical qPCR profile for a DNA library containing a random 40-nt region flanked by two 20-nt constant primer regions showing unexpected result inconsistent with automated analysis.

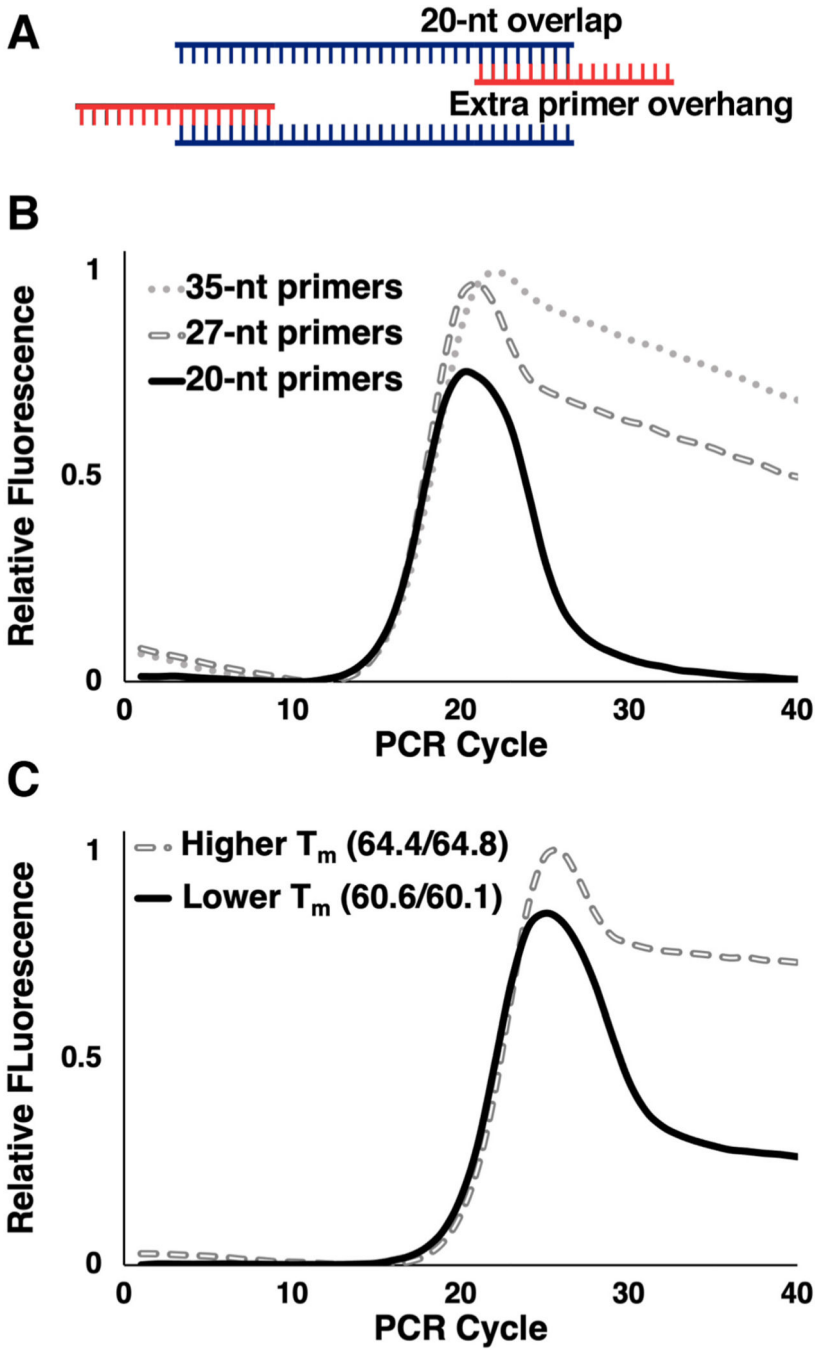

Fig. 2.

A) Schematic depiction of primers designed to anneal to 20-nt fixed sequences flanking template random region and indicating addition of 5′ overhangs to lengthen PCR products. B) qPCR profiles for various primers (20-nt, no overhang; 27-nt, 7-nt overhang; 35 nt, 15-nt overhang) with a $20(N_{40})20$ template. C) Moderate qPCR profile improvement for 27-nt primer pairs with ($T_{m,\ forward}$/$T_{m,\ reverse}$) indicated in °C.

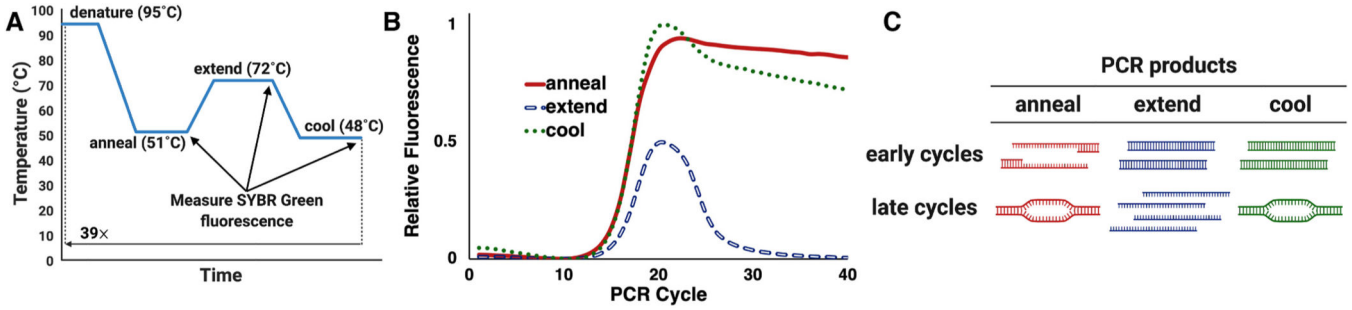

Fig. 3.

A) Detection of SYBR Green fluorescence after each of three steps: anneal (51 °C), extend (72 °C), and cool (48 °C). B) SYBR Green qPCR profiles monitored for the same reaction after these three steps: extend (blue), cool (green), and anneal (red). C) Interpretation of qPCR product complexes detected at early and late cycles for DNA libraries containing a central N_{40} random region.

Table 1

Interpretability of qPCR profiles for experimental DNA templates.

Template[a]	Forward primer length (T_m)/Reverse primer length (T_m)[b]	Extension[c]	Cooling[c]	Annealing[c]
20(40)20	20(52.7)/20(55.6)	++	++	++
20(40)20	20(52.7)/20(55.7)	++	++	++
20(40)20	27(60.6)/27(60.1)[d]	++	++	++
27(40)26	27(63.1)/26(65.1)	++	++	++
20(40)20	27(64.1)/27(65)[d]	++	++	++
20(40)20	27(64.4)/27(64.8)[d]	++	++	++
20(40)20	35(67)/35(66.9)[d]	++	++	++
20(N_{40}) 20	20(52.7)/20(55.6)	–	+	++
20(N_{40}) 20	20(52.7)/20(55.7)	–	+	++
20(N_{40}) 20	27(60.6)/27(60.1)[d]	–	+	++
27(N_{40}) 26	27(63.1)/26(65.1)	+	+	++
20(N_{40}) 20	27(64.1)/27(65)[d]	+	+	++
20(N_{40}) 20	27(64.4)/27(64.8)[d]	+	+	++
20(N_{40}) 20	35(67)/35(66.9)[d]	+	+	++

[a] Structure of template is presented as left flanking region length (central region length) right flanking region length, where lengths are in nt. Random central regions indicated by N.

[b] Lengths in nt. Calculated T_M values in °C. For primers with overhangs the calculated T_M values are for the full-length binding.

[c] Point in PCR cycle where fluorescence is interrogated, with resulting curve profile indicated as (−): uninterpretable non-sigmoid curve; (+) poorly interpretable partial sigmoid curve; (++) easily interpretable sigmoid curve.

[d] Primer sets with extra primer overhang as shown in Fig. 2.